

Original Research Article

Biogenic synthesis of silver nanoparticles from waste banana plant stems and their antibacterial activity against *Escherichia coli* and *Staphylococcus Epidermis*

Huu Dang, Derek Fawcett, Gerrard Eddy Jai Poinern*

Department of Physics, Energy Studies and Nanotechnology, School of Engineering and Energy, Murdoch University, Murdoch, Western Australia 6150, Australia

Received: 20 June 2017

Accepted: 18 July 2017

*Correspondence:

Dr. Gerrard Eddy Jai Poinern,

E-mail: g.poinern@murdoch.edu.au

Copyright: © the author(s), publisher and licensee Medip Academy. This is an open-access article distributed under the terms of the Creative Commons Attribution Non-Commercial License, which permits unrestricted non-commercial use, distribution, and reproduction in any medium, provided the original work is properly cited.

ABSTRACT

Background: This study for the first time presents an eco-friendly and room temperature procedure for biologically synthesizing silver (Ag) nanoparticles from waste banana plant stems.

Methods: A simple and straightforward green chemistry based technique used waste banana plant stems to act as both reducing agent and capping agent to produce Ag nanoparticles, which were subsequently characterized. In addition, antibacterial studies were conducted using the Kirby-Bauer sensitivity method.

Results: Advanced characterisation revealed the Ag nanoparticles had a variety of shapes including cubes, truncated triangular and hexagonal plates, and ranged in size from 70 nm up to 600 nm. The gram-negative bacteria *Escherichia coli* showed the maximum inhibition zone of 12 mm.

Conclusions: The study has shown that waste banana plant stems can generate Ag nanoparticles with antibacterial activity against *Escherichia coli* and *Staphylococcus epidermis*.

Keywords: Agricultural waste, Antibacterial, Biogenic synthesis, Silver nanoparticles

INTRODUCTION

Throughout antiquity silver (Ag) was valued as a precious metal and accordingly was used in a variety of applications such as jewellery, decorations and currency. One of the earliest medicinal uses for Ag was recorded almost 2500 years ago when Herodotus described the king of Persia ordering the boiling of water prior to its storage in silver flagons before going to war.^{1,2} In 1869, Raulin reported the first modern antimicrobial based description for describing the effects of Ag against the growth of water based *Aspergillus niger* in Ag storage vessels.³ Recently, nanotechnology-base processes have been extensively used to manufacture noble metal nanoparticles for biomedical applications.^{4,5} In particular,

Ag nanoparticles have attracted considerable interest due to their unique biological, electrical and optical properties.⁶⁻⁹

Current medical research has shown that Ag nanoparticles are effective antibacterial agents and can be used to induce cell apoptosis in some forms of cancer.¹⁰⁻¹² The antimicrobial properties are believed to stem from the nanoparticles size, shape and surface chemistry that interact and damage cell membranes.^{13,14} Because of the toxicity towards microbes, future Ag nanoparticle-based pharmaceutical products are planned and some are currently under development.^{15,16} It is for this reason that many researchers are currently investigating new synthesis techniques for producing Ag nanoparticles with

programmable parameters such as size, shape and surface chemistry.¹⁷

Traditional physical and chemical processes used to manufacture metallic nanoparticles are not eco-friendly, since they use toxic chemicals and solvents during formation and subsequent nanoparticle stabilisation. Therefore, to avoid the disadvantages associated with traditional manufacturing processes new green chemistry-based procedures using biological entities such as bacteria, fungi, yeast, and plant extracts are currently under investigation.¹⁸⁻²¹

Among the alternatives, the use of plant extracts offers a straight-forward, clean and eco-friendly method of producing noble nanoparticles such as Au and Ag.^{22,23} However, very little research has been done investigating the possible utilization of naturally occurring agricultural plant wastes for the biogenic synthesis of Ag nanoparticles. For example, banana plants are extensively cultivated around the world and can grow to heights of several metres. They are the biggest plants on earth without a woody stem, and their appearance resembles that of a tree with stem diameters reaching around 60 cm. At harvest, fruit bearing branches are removed and the remaining plants are cut down to produce very large quantities of waste.

Australia for example produces around 340,000 tonnes of bananas each year generating a revenue of around AUS \$550 million, but there is no data regarding the vast amount of plant waste tonnage produced by harvesting.²⁴ Thus, to better utilise plant wastage produced by the global banana industry, a small number of studies have investigated using the biomolecules present in banana fruit peel to generate Ag nanoparticles.²⁵ However, to date there are no articles reporting the use of waste banana plant stems for the biogenic synthesis of Ag nanoparticles.

The present study, for the first time uses extracts taken from banana plant stems to produce high value Ag nanoparticles with antimicrobial properties. The room temperature procedure begins by mixing a banana stem extract with an aqueous solution of AgNO₃. During reduction, the colour of the reaction mixture became brown indicating the formation of Ag nanoparticles. The resulting Ag nanoparticles were subsequently characterised using UV-visible spectroscopy, X-ray diffraction analysis, energy dispersive spectrometer (EDS) analysis and scanning electron microscopy (SEM). Furthermore, the antibacterial properties of the Ag nanoparticles towards *Escherichia coli* and *Staphylococcus Epidermis* via the Kirby-Bauer sensitivity method.²⁶

METHODS

The source of the Ag⁺ ions was silver nitrate [AgNO₃, (99.99%)] and the capping agent used was sodium citrate

[C₆H₅Na₃O₇, (99.99%)]. Both chemicals were supplied by Sigma-Aldrich (Castle Hill, NSW Australia). All aqueous solutions used in this study were made from Milli-Q[®] water produced by an Ultrapure Water System (D11931 Barnstead, 18.3 MΩ cm⁻¹) supplied by Thermo scientific.

The banana (*Musa acuminata* or commonly called Cavendish group) stems were randomly selected from a representative selection of plants. The stems were washed, diced and then a 1 g sample of the diced matter was added to glass beaker containing 100 mL of Milli-Q[®] water. The mixture was then heated at 75°C for 1 hour before being allowed to slowly cool down to room temperature (22 °C). After cooling, the aqueous mixture was filtered using a 0.22 μm Millex[®] (33 mm Dia.) syringe filter. The filtered extract (BE) was then transferred to 250 mL Schott bottle for storage before being used in the synthesis procedure.

Biogenic synthesis of Ag nanoparticles

The procedure consisted of a two-step process. The first step consisted of adding a 1 mL aqueous solution of 0.1 M AgNO₃ to a glass vial containing a 1 mL aqueous solution of 0.1 M C₆H₅Na₃O₇. The solutions were mixed for 1 minute and then allowed to stand. The Ag nanoparticles formed during this step were used as a control in the antibacterial study. In the second step, a 1 mL aqueous solution of 0.1 M AgNO₃ was added to glass vials containing varying quantities of BE (1, 5, 10, 15, and 20 mL) designated as b1, b2, b3, b4 and b5 respectively as seen in (Figure 1). After an initial mixing period 2 minutes, the reduction process could progress at room temperature (22°C) Figure 1.

Advanced characterization

All samples were investigated using UV-visible spectroscopy, x-ray diffraction, energy dispersive spectroscopy (EDS) and scanning electron microscopy (SEM). The biogenic synthesis of Ag⁺ ions in the respective samples was monitored at room temperature using UV-visible spectroscopy (Varian Cary 50 series UV-Visible spectrophotometer V3) over a spectral range between 200 and 800 nm, with a spectral resolution a 1 nm. XRD analysis was carried to identify the presence of metallic Ag in the respective samples using a Bruker D8 series diffractometer using flat plane geometry over a 2 second acquisition time.

The diffractometer operated at 40 kV and 30 mA (Cu Kα = 1.5406 Å radiation source) and collected data over a 2θ range between 15° and 80° with an incremental step size of 0.04°. SEM images were produced by a JEOL JCM-6000, NeoScopeTM microscope. The images were used to determine particle size and morphology. While the attached EDS spectrometer unit was used to detect the presence of Ag and identify other elements present in the samples.

Samples for imaging were first dried and then attached to holders using carbon adhesive tape prior to receiving a 2-nm layer of gold up using a sputter coater (Cressington 208HR) to prevent charge build up.

Antibacterial activity of Ag nanoparticles

Nanoparticle antibacterial activity was evaluated using the sensitivity method of Kirby-Bauer.²⁶ Two bacterial strains (*Escherichia coli*; gram-negative and *Staphylococcus Epidermis*; gram-positive) were used in the antibacterial challenge. The sub-cultured bacteria were swabbed uniformly over a nutrient agar medium contained in a 90 mm diameter Petri dishes using a sterile cotton swab. Then 50 μ L nanoparticle sample solutions were deposited on sterile disks (6 mm Whatman® AA 2017-006) using a micropipette. The disks were air dry for 20 minutes before being placed on the respective bacteria treated agar plates using sterile forceps. The plates were then incubated at 37 °C for 48 h. After incubation, the zone of inhibition of the various samples were measured, compared and the antibacterial performance of each evaluated.

RESULTS

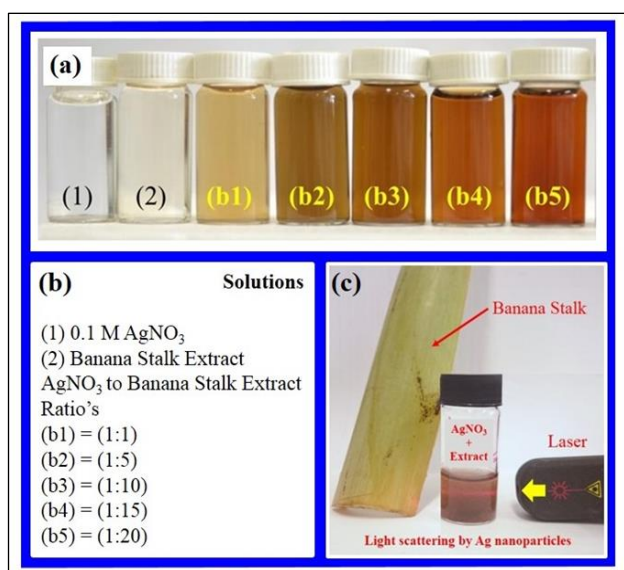


Figure 1: (a) Appearance of pure and mixture solutions; (b) solution ratios, and (c) Ag nanoparticles detected by laser light scattering.

Visual inspection of samples revealed that a colour change occurred during in all reaction mixtures (b1 to b5) as seen in (Figure 1 a). The colour change was credited to the excitation of the surface plasmon resonance (SPR) of the forming Ag nanoparticles in the respective reaction mixtures. The nanoparticles were detected in the respective reaction mixtures by the scattering of laser light as seen in (Figure 1 c). UV-visible absorption spectroscopy was used to investigate the SPR of the various reaction mixtures. (Figure 2) presents

representative UV-visible spectra for samples (b1), (b4) and (b5) along with their respective visual images showing their characteristic brownish-orange colour. The SPR occurred at 430 nm for the samples as seen in (Figure 2).

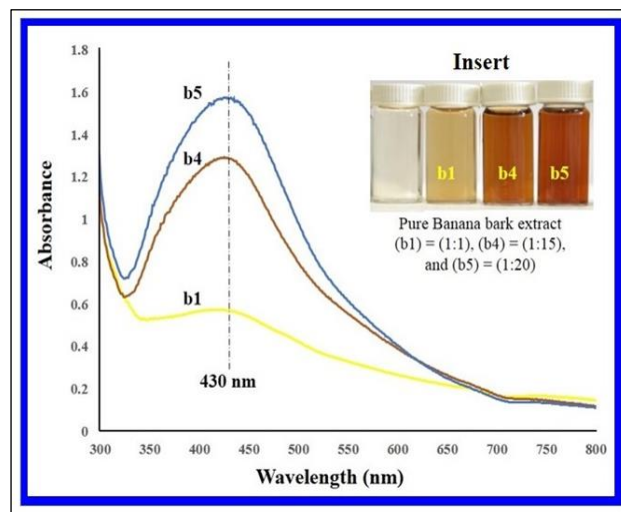


Figure 2: UV-visible spectroscopy analysis of Ag nanoparticles synthesized from various ratios of banana stem extracts and corresponding reaction mixture COLORS.

(Figure 3 a) presents a representative SEM image of Ag nanoparticles formed from a b2 (1:5) reaction mixture. In addition to spherical Ag nanoparticles are many cubes (red arrows) and triangular plates (yellow arrows) present. Spheres range in size from 70 nm up to 250 nm, cubes range in size from 80 nm up to 300 nm and triangular plates ranges in size from 80 nm up to 600 nm. Triangular plates are few compared to cubes, but tend to be larger. (Figure 3 b) presents an enlarged image of a single triangular Ag nanoparticle with a side length of 600 nm. The XRD pattern presented in (Figure 3 c) reveals

Bragg reflection peaks located at 37.7°, 45.0°, 65.0° and 77.0° in the 2 θ range between 10° to 80°. The peaks were indexed as (111), (200), (220) and (311) planes respectively and are consistent with a face centered cubic structure associated with the standard diffraction pattern of JCPDS No 89-3722 for Ag. The intensity of the peak corresponding to the (111) plane is slightly greater than other peaks in the patterns and suggests the plane is the predominant orientation. Also present in the pattern is a peak located at 32.0°, which corresponds to the (111) plane and was indexed as Ag₂O.

The strong elemental signal for Ag in the EDS analysis confirmed the presence of elemental Ag in the samples as seen in (Figure 3 d). Also in the representative analysis were peaks for Aluminum (from the SEM stub), silicon (from the mica substrate), carbon (from the carbon tape used to fix the samples) and gold used to coat the

samples. Also present was an oxygen peak, which is believed to be responsible for the Ag₂O detected in the XRD studies.

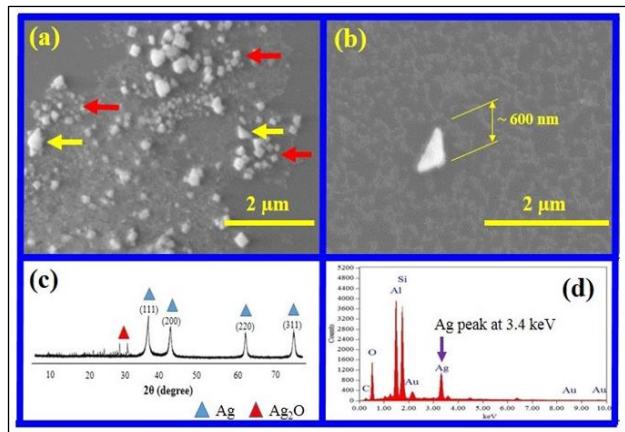


Figure 3: (a) Representative SEM image of synthesized Ag nanoparticles; (b) enlarged image of triangular particle; (c) XRD pattern showing the presence of crystalline Ag, and (d) EDS confirmation of metallic Ag present in samples.

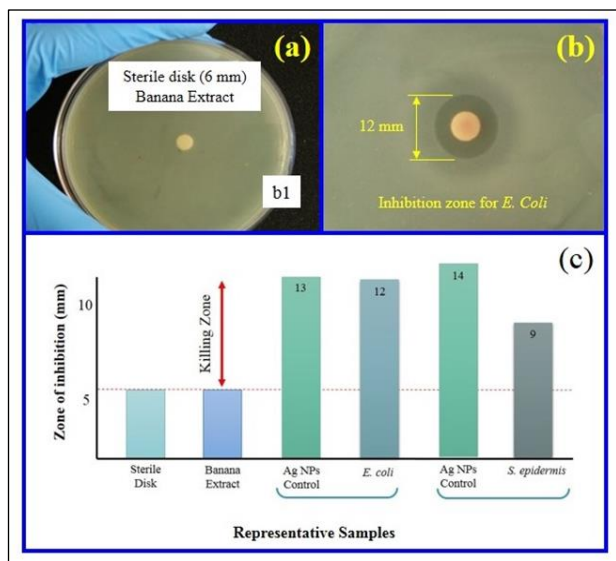


Figure 4: (a) A representative petri dish sample of sterile disk and banana extract sample (b1); (b) *Escherichia coli* being challenged by leaf extract mediated Ag nanoparticles, and (c) representative results for the antibacterial challenge.

The antibacterial challenge found disks treated with pure banana extracts produced a null result. Thus, indicating the banana extracts had no antibacterial effect against *Escherichia coli* and *Staphylococcus Epidermis*. Chemically generated Ag nanoparticles (control) were challenged by both bacteria. The mean inhibition zone for *Escherichia coli* was estimated to be 13 mm, while the mean inhibition zone for *Staphylococcus Epidermis* was found to be 10 mm. Next, Ag nanoparticles generated and

suspended in the banana extract (b1) were challenged by the bacterial strains. *Escherichia coli* recorded a mean inhibition zone of 12 mm and *Staphylococcus Epidermis* a mean value of 9 mm. A representative antibacterial test dish containing a disk treated with banana extract (b1) is presented in (Figure 4 a) and reveals a null result. While (Figure 4 b) shows a representative inhibition, zone produced by Ag nanoparticles contained within a banana extract (b1) against *Escherichia coli*. Results of the antibacterial challenge are graphically presented in (Figure 4 c) and indicate inhibition zones for Ag nanoparticles generated by a banana extract were smaller than chemically produced Ag nanoparticles.

DISCUSSION

UV-visible absorption spectroscopy was used to investigate the SPR of reaction mixtures with varying amounts of banana extract. Higher ratios of extract in the reaction mixture produced more pronounced single peaks as seen in (Figure 2) and increasing darkness of the brownish-orange mixture as seen in (Figure 1 a). Inspection of (Figure 2) revealed that the SPR occurred at 430 nm for the representative samples. Mie's theory predicts a single SPR band in the absorption spectra for spherical metal nanoparticles, while anisotropic particles would produce two or more SPR bands.^{27,28}

Thus, the UV-visible spectra indicate spherical Ag nanoparticles were initially formed. Similar results have been reported by other researchers for other plant extracts used for the biogenic synthesis of Ag nanoparticles. For example, Ahmad and Sharma have used *Ananas comosus* (Pineapple) extract to generate spherical Ag nanoparticles ranging in size from 5 to 35 nm.²⁹ Similarly, Konwarha et al, have generated spherical-shaped Ag nanoparticles ranging in size from 3 to 12 nm using an extract taken from *Citrus sinensis* (Orange) peel.³⁰ While Basavegowda et al, have used an extract taken from *Citrus unshiu* (Mandarin) peel to generate spherical Ag nanoparticles ranging in size from 5 to 20 nm.³¹

However, the study did find that for periods greater than 20 minutes particle morphology changed from spherical to cubical and triangular as seen in (Figures 3 a and b). The crystalline structure of the Ag nanoparticles was confirmed by XRD spectroscopy (Figure 3 c) and the presence of Ag in the samples was also confirmed by EDS analysis (Figure 3 d). Analysis of XRD data revealed the Ag nanoparticles had a face centred cubic structure (JCPDS No 89-3722) and is similar to the results of other researchers.³²⁻³⁴ Thus, characterisation studies confirmed banana plant stem extracts could be used to generate crystalline Ag nanoparticles.

The antibacterial properties of the Ag nanoparticles were evaluated using the sensitivity method of Kirby-Bauer. Initially, untreated sterile pads were challenged by the respective cultured bacterial strains in Petri dishes. As expected, the test confirmed no antibacterial properties

were produced by the sterile disks and accordingly established a baseline for inhibition zone measurements. The next step evaluated disks treated with pure banana plant stem extracts, which subsequently produced a null result for both bacterial strains.

A similar study by Ibrahim revealed banana peel extracts also produced no antibacterial properties towards several bacterial strains including *Escherichia coli*.³⁵ Next, chemically synthesised Ag nanoparticles (control) were challenged by the bacterial strains. The inhibition zones were recorded (*Escherichia coli*; 13 mm, and *Staphylococcus Epidermis*; 14 mm), the measurements were then used as a comparison between the respective banana stem extracts. The control measurements were similar between the bacterial strains, with *Staphylococcus Epidermis* being slightly more susceptible to the control Ag nanoparticles as seen in (Figure 4 c). The respective bacterial strains were then challenged with biologically synthesised Ag nanoparticles. After the challenge, the inhibition zones were measured.

Inspection of a representative set antibacterial challenges for the b1 sample revealed inhibition zones for all bacterial strains were smaller to the control Ag nanoparticles (*Escherichia coli*; 12 mm, and *Staphylococcus Epidermis*; 9 mm). This difference between inhibition zone sizes can be seen in (Figure 4 c) for the b1 sample. The size difference seen for *Escherichia coli* was 1 mm, while the difference for *Staphylococcus Epidermis* was 5 mm. The difference between chemically produced and biologically synthesis Ag nanoparticles has also been reported by Kokila et al, for banana peel extract.³⁶

The present study revealed *Escherichia coli* (gram-negative) displayed a larger inhibition zone compared with *Staphylococcus Epidermis* (gram-positive). The most likely cause for this difference is due to the variation in cell wall composition of the two-gram types. Gram-positive bacteria have a rigid cell wall structure, which is composed of a thick peptidoglycan layer composed of linear polysaccharide chains. These chains are cross linked by short peptides. Thus, making it difficult for Ag nanoparticles to penetrate the cell wall. While the much thinner peptidoglycan layer of gram-negative bacteria offers less resistance to Ag nanoparticles penetrating the cell wall.³⁷

Studies have suggested that there are three main mechanisms that underlie the antibacterial properties of Ag nanoparticles: 1) Ag nanoparticles attach to negatively charges cell wall, change the walls physiochemical properties and disrupt cell functions such as permeability, respiration and osmoregulation; 2) permeating Ag nanoparticles interact and disrupt DNA, proteins and other cell constituents, and 3) Ag nanoparticles act as reservoirs for the release of Ag⁺ ions (bactericidal agent) that enhances the antibacterial effect.³⁸⁻⁴⁵ Differences in the size of the inhibition zones

of control and biologically synthesised Ag nanoparticles is believed to result from residual biomolecules coating the nanoparticle surface.

The surface coating or corona appears to moderate the antibacterial properties and reduce the effectiveness of the biologically synthesised Ag nanoparticles.⁴⁶ In addition, nanoparticle sizes can also be smaller than assessed, since the measured size also includes biomolecules covering the core Ag nanoparticle.⁴⁷ Thus, some degree of caution needs to be taken when comparing sizes and chemical reactivity of nanoparticles produced by traditional chemical techniques and those produced by biological synthesis.⁴⁸

CONCLUSION

The present work banana plant stems, an agricultural waste material, was used for the biogenic synthesis of high value Ag nanoparticles. The study has shown that a natural, renewable and low-cost waste material can be effectively used as a biological reducing agent. The room temperature approach is cost-effective, non-toxic, and an eco-friendly alternative to traditional physical and chemical manufacturing processes.

The Ag nanoparticles produced by this green approach were characterized and found to be stable and crystalline. They had a face centered cubic structure, had three shapes and ranged in size from 70 nm up to 600 nm. Spheres were between 70 nm and 250 nm, cubes were between 80 nm and 300 nm and triangular plates were between 80 nm and 600 nm. The Ag nanoparticles displayed good antibacterial activity against *Escherichia coli* and *Staphylococcus Epidermis*, with *Escherichia coli* (gram-negative) being the most susceptible with an inhibition zone of 12 mm. However, further studies are needed to investigate the influence of residual biomolecules deposited on the Ag nanoparticles during biological synthesis on bacterial strains.

ACKNOWLEDGEMENTS

Authors would like to thank Dr. Mona Shah and Mrs. Purabi Ghosh for their assistance with antibacterial studies. This work was partly supported by Horticulture Innovation Australia Project A114003 and Derek Fawcett would like to thank Horticulture Innovation Australia for their research fellowship.

Funding: No funding sources

Conflict of interest: None declared

Ethical approval: Not required

REFERENCES

1. The History of Herodotus, EH Blakeney, Editor, translated by G. Rawlinson, J.M. Dent and Sons Ltd, London, UK, 1945.

2. Sykes, G, Disinfection and Sterilization, Publisher: E. and F. N. Spon Ltd., London, UK, 1958.
3. Raulin J. Chemical studies on growth. *Ann Sci Nat Bot.* 1869;11:93-299.
4. Lee KS, El-Sayed MA. Gold and silver nanoparticles in sensing and imaging: sensitivity of plasmon response to size, shape, and metal composition. *J Phys Chem B.* 2006;110:19220-5.
5. Jain PK, Huang X, El-Sayed IH, EL-Sayed MA. Noble metals on the nanoscale: optical and photothermal properties and some applications in imaging, sensing, biology, and medicine. *Acc Chem Res.* 2008;41:1578-86.
6. Setua P, Chakraborty A, Seth D, Bhatta MU, Satyam PV, Sarkar N. Glucosamine-functionalized silver glycol nanoparticles: characterization and antibacterial activity. *J Phys Chem C.* 2007;111:3901-7.
7. Manno D, Filippo E, Di Giulio M, Serra A. Synthesis and characterization of starch-stabilized Ag nanostructures for sensors applications. *J Non-Crystalline Solids.* 2008;354(52-54):5515-20.
8. Chen X, Schluesener HJ. Nanosilver. A nanoparticle in medical applications. *Toxicol Letters.* 2008;176 (4):1-12.
9. Nair LS, Laurencin CT. Silver nanoparticles: synthesis and therapeutic applications. *J Biomed Nanotechnol.* 2007;3:301-16.
10. Sondi I, Salopek-Sondi B. Silver nanoparticles as antimicrobial agent: a case study on *E. coli* as a model for Gram negative bacteria. *J Colloid Interface Sci.* 2004;275(1):177-82.
11. Kim JS, Kuk E, Yu KN, Kim JH, Park SJ, Lee HJ, et al. Antimicrobial effects of silver nanoparticles. *Nanomedicine.* 2007;3(1):95-101.
12. Sanpui P, Chattopadhyay A, Ghosh SS. Induction of apoptosis in cancer cells at low silver nanoparticle concentrations using chitosan nanocarrier. *ACS Appl Mater Interfaces.* 2011;3(2):218-28.
13. Brayner R, Ferrari-Iliou R, Brivois N, Djediat S, Benedetti M, Fievet F. Toxicological impact studies based on *Escherichia coli* bacteria in ultrafine ZnO nanoparticles colloidal medium. *Nano Letters.* 2006;6:866-70.
14. Simon-Deckers A, Loo S, Mayne-L'hermite M, Herlin-Boime N, Menguy N, Reynaud C, Gouget B, et al. Size composition and shape dependent toxicological impact of metal oxide nano-particles and carbon nano-tubes toward bacteria. *Environmental Sci Technol.* 2009;43:8423-9.
15. Choi O, Deng KK, Kim NJ, Ross Jr L, Surampalli RY, Hu Z. The inhibitory effects of silver nanoparticles, silver ions, and silver chloride colloids on microbial growth. *Water Res.* 2008;42:3066-74.
16. Rai M, Yadav A, Gade A. Silver nanoparticles as a new generation of antimicrobials. *Biotechnol Adv.* 2009;27:76-83.
17. Panigrahi S, Kundu S, Ghosh SK, Nath S, Pal T. General method of synthesis for metal nanoparticles. *J Nanoparticle Res.* 2004;6(4):411-4.
18. Shah M, Fawcett D, Sharma S, Tripathy S, Poinern GEJ. Green synthesis of metallic nanoparticles via biological entities. *Materials.* 2015;8:7278-308.
19. Poinern GEJ, Le X, Chapman P, Fawcett D. Green biosynthesis of gold nanoparticles using the leaf extracts from an indigenous Australian plant *Eucalyptus macrocarpa*. *Gold Bulletin.* 2013;46:165-73.
20. Kulkarni N, Muddapur U. Biosynthesis of metal nanoparticles: A review. *J Nanotechnol.* 2014:1-8.
21. Mittal AK, Chisti Y, Banerjee UC. Synthesis of metallic nanoparticles using plants. *Biotechnol Advances.* 2013;31:346-56.
22. Nellore J, Pauline PC, Amarnath K. Biogenic synthesis of *Sphearanthus amaranthoids* towards the efficient production of the biocompatible gold nanoparticles. *Dig J Nanomater Biostruct.* 2012;7:123-33.
23. Singh PP, Bhakat C. Green synthesis of gold nanoparticles and silver nanoparticles from leaves and bark of *Ficus carica* for nanotechnological applications. *Int J Sci Res Pub.* 2012;2:1-4.
24. Retrieved from <http://www.freshplaza.com/sector/157/australia-new-zealand> 2016, Oct 12.
25. Banker A, Joshi B, Kumar AR, Zinjarde S. Banana peel extract mediated novel route for the synthesis of silver nanoparticle. *Colloids and Surfaces A: Physiochem Eng Aspects.* 2010;368:58-63.
26. Jorgensen JH, Turnidge JD. Susceptibility test methods: dilution and disk diffusion methods. In: Murray PR, Baron EJ, eds. *Manual of clinical microbiology*, 9th ed. ASM Press, Washington DC; 2007:1152-1172.
27. He R, Qian X, Yin J, Zhu Z. Preparation of polychrome silver nanoparticles in different solvents. *J Mater Chem.* 2002;12:3783-6.
28. Novak JP, Feldheim DL. Assembly of phenylacetylene bridged silver and gold nanoparticle arrays. *J Am Chem Soc.* 2000;122:3979-80.
29. Ahmad N, Sharma S. Green Synthesis of Silver Nanoparticles Using Extracts of *Ananas comosus*. *Green Sustainable Chemistry.* 2012;2:141-7.
30. Konwarh R, Gogoi B, Philip R, Laskar MA, Karak N. Biomimetic preparation of polymer-supported free radical scavenging, cytocompatible and antimicrobial 'green' silver nanoparticles using aqueous extract of *Citrus sinensis* peel. *Colloids and Surfaces B: Bio-interfaces.* 2011;84:338-45.
31. Basavegowda N, Rok Lee Y. Synthesis of silver nanoparticles using Satsuma mandarin (*Citrus unshiu*) peel extract: a novel approach towards waste utilization. *Mater Lett.* 2013;109:31-3.
32. Dwivedi AD, Gopal K. Plant-mediated biosynthesis of silver and gold nanoparticles. *J Biomed Nanotechnol.* 2011;7:163-4.

33. Edison TJI, Sethuraman M. Instant green synthesis of silver nanoparticles using *Terminalia chebula* fruit extract and evaluation of their catalytic activity on reduction of methylene blue. *Process Biochem.* 2012;47:1351-7.
34. Shah M, Poinern GEJ, Fawcett D. Biosynthesis of silver nanoparticles using indigenous *Xanthorrhoea glauca* leaf extract and their antibacterial activity against *Escherichia coli* and *Staphylococcus epidermis*. *Int J Res Med Sci.* 2016;4:2886-92.
35. Ibrahim HMM. Green synthesis and characterization of silver nanoparticles using banana peel extract and their antimicrobial activity against respective microorganisms. *J Radiation Applied Sci.* 2015;8:265-75.
36. Kokila T, Ramesh PS, Geetha D. Biosynthesis of silver nanoparticles from Cavendish banana peel extract and its antibacterial and free radical scavenging assay: a novel biological approach. *Appl Nanosci.* 2015;5(8):911-20.
37. Shrivastava S, Bera T, Roy A, Singh G, Ramachandrarao P, Dash D. Characterization of enhanced antibacterial effects of novel silver nanoparticles. *Nanotechnol.* 2007;18:103-12.
38. Dibrov P, Dzioba J, Gosink KK, Hase CC. Chemiosmotic Mechanism of Antimicrobial Activity of Ag? In *Vibrio cholera* Antimicrob. Agents Chemother. 2002;46:2668-70.
39. Sondi I, Salopek-Sondi B. Silver nanoparticles as antimicrobial agent: a case study on *E. coli* as a model for gram-negative bacteria. *J Colloid Interface Sci.* 2004;275:177-82.
40. Nel AE, Madler L, Velegol D, Xia T, Hoek EMV, Somasundaran P, et al. Understanding biophysicochemical interactions at the nano-bio interface. *Nature Materials.* 2009;8:543-57.
41. Su HL, Chou CC, Hung DJ, Lin SH, Pao IC, Lin JH, et al. The disruption of bacterial membrane integrity through ROS generation induced by nanohybrids of silver and clay. *Biomaterials.* 2009;30:5979-87.
42. Marambio-Jones C, Hoek EMV. A review of the antibacterial effects of silver nanomaterials and potential implications for human health and the environment. *J Nanoparticle Res.* 2010;12:1531-51.
43. AshaRani PV, Mun GLK, Hande MP, Valiyaveetil S. Cytotoxicity and genotoxicity of silver nanoparticles in human cells. *ACS Nano.* 2009;3:279-90.
44. Subhasree B, Baskar R, Laxmi Keerthana R, Susan RL, Rajasekaran, P. Evaluation of antioxidant potential in selected green leafy vegetables. *Food Chem.* 2009;115(4):1213-20.
45. Liu JY, Sonshine DA, Shervani S, Hurt RH. Controlled release of biologically active silver from nanosilver surfaces. *ACS Nano.* 2010;4:6903-13.
46. Fawcett D, Verduin JJ, Shah M, Sharma SB, Poinern GEJ. A Review of Current research into the biogenic synthesis of metal and metal oxide nanoparticles via marine algae and seagrasses. *J Nanoscience.* 2017:1-15.
47. Prathna TC, Chandrasekaran N, Raichur M, Mukherjee A. Biomimetic synthesis of silver nanoparticles by Citrus limon (lemon) aqueous extract and theoretical prediction of particle size. *Colloid Surf. B Biointerface.* 2011;82:152-9.
48. Kasthuri J, Veerapandian S, Rajendiran N. Biological synthesis of silver and gold nanoparticles using apiin as reducing agent. *Colloid Surf. B Biointerface.* 2009;68:55-60.

Cite this article as: Dang H, Fawcett D, Poinern GEJ. Biogenic synthesis of silver nanoparticles from waste banana plant stems and their antibacterial activity against *Escherichia coli* and *Staphylococcus Epidermis*. *Int J Res Med Sci* 2017;5:3769-75.